Morad, Omar; Viitala, Raine; Saikko, Vesa

Behavior of marine thruster lip seals under typical operating conditions

Published in:
Tribology International

DOI:
10.1016/j.triboint.2024.110195

Published: 01/01/2025

Document Version
Publisher's PDF, also known as Version of record

Tribology International 201 (2025) 110195

Contents lists available at ScienceDirect

Tribology International

journal homepage: www.elsevier.com/locate/triboint

Behavior of marine thruster lip seals under typical operating conditions

Omar Morad *, Raine Viitala, Vesa Saikko

Aalto University School of Engineering, Finland

ARTICLE INFO

Keywords:
Lip seal
Marine lip seals
NBR

ABSTRACT

Marine thruster lip seals pose a condition monitoring challenge, yet they are seldom studied tribologically. The present work studies the behavior of a 300 mm diameter NBR marine thruster lip seal (n = 3) under typical operating conditions. Frictional torque and subsurface temperature were measured under 27 combinations of oil temperature, oil pressure, and rotational speed. The frictional torque increased with increasing oil pressure and decreased with increasing oil temperature. The subsurface temperature increased with increasing oil temperature, oil pressure, and rotational speed. There was no clear relation between the frictional torque and subsurface temperature. The frictional torque ranged 9.6–14.4 Nm, and subsurface temperature 57–94 °C. Preliminary wear measurements showed a wear track width of 0.2–0.3 mm and a wear rate of 0.031 ± 0.001 mm^3/hour.

1. Introduction

Rotary lip seals are widely used in many technical fields, one of which is the marine field. Marine lip seals are critical components for ships since they seal the marine thruster gearbox lubricant and gears from seawater, debris, or contaminants. Therefore, their failure may lead to significant oil leakage to the sea, or seawater leakage to the gearbox, which may result in significant mechanical damage to the gearbox. Furthermore, replacing marine lip seals requires dry-docking the ship, which is an expensive and time-consuming process. A routine dry docking takes place every five years as a part of a mandatory major service for marine vessels, during which the seals are replaced. Since replacing marine seals requires dry docking, an unexpected seal failure during normal operation results in additional costs and vessel downtime, which marine vessel operators desire to avoid. Lip seals may also leak during operation, which is a minor mechanical issue but a major environmental one. Oil leakage during regular operation of lip seals is estimated to be 1–10 liters per day for a single thruster [1].

A marine lip seal package typically consists of three to five lip seals of the same size, such as the package shown in Fig. 1, which has three lip seals. Multiple lip seals are used to prevent the oil and water from mixing since a single lip seal does not separate fluids [2,3]. The direction of each seal in the package is chosen according to the design philosophy and the role of the seal. For instance, in Fig. 1, the leftmost seal has seawater on the spring side, so it seals the seawater from the oil, but seawater may leak past this seal due to fluid mixing. The middle seal acts as an additional barrier to stop the seawater from leaking further towards the gearbox. The rightmost seal has the gearbox cavity on its backside, and a supply of barrier oil on its spring side. The barrier oil is the same as the gearbox oil, and is typically supplied to the spring side of the rightmost seal at a higher pressure than seawater and gearbox cavity oil. This ensures sufficient radial force for the seal during regular operation, and acts as a barrier in case of critical seal failure, flowing towards both the gearbox cavity and the middle seal. The middle seal has two roles; it seals the barrier oil and prevents it from flowing to the sea, and acts as a redundant seal in case the rightmost seal fails. If the middle seal fails, the higher pressure of the barrier oil may cause the leftmost seal to lift off, resulting in constant leakage. This is designed as a less critical mode of seal failure since it prevents seawater ingress to the gearbox.

A lip seal works by way of the reverse pumping mechanism, proposed by Müller [4] and Qian [5]. When the shaft rotates, it deforms the contact width of the lip seal tangentially, deforming the asperities at the contact to form an asymmetric V-shape. The asymmetric deformation of the asperities causes them to act as two opposite vane pumps. As a result, two axial oil flows are produced, one to either side of the lip seal. The net oil flow in a successful seal is towards the spring side, i.e., towards the sealed fluid. The rotation of the shaft also drags the oil at the contact over the asperities, creating tangential oil flow, which increases the local oil pressure and generates a lubricant film between the lip and the shaft.

There have been numerous numerical models of lip seal behavior, with varying degrees of complexity and experimental agreement. The first of such models [6–8] were published with the advancement of computing power, where a constant film thickness was assumed. The models consisted of solid mechanics and fluid dynamics analyses. The

* Correspondence to: Aalto University School of Engineering, Department of Mechanical Engineering, PO Box 14400, FI-00076 Aalto, Finland.
E-mail address: omar.morad@aalto.fi (O. Morad).

https://doi.org/10.1016/j.triboint.2024.110195
Received 23 May 2024; Received in revised form 31 August 2024; Accepted 1 September 2024
Available online 3 September 2024

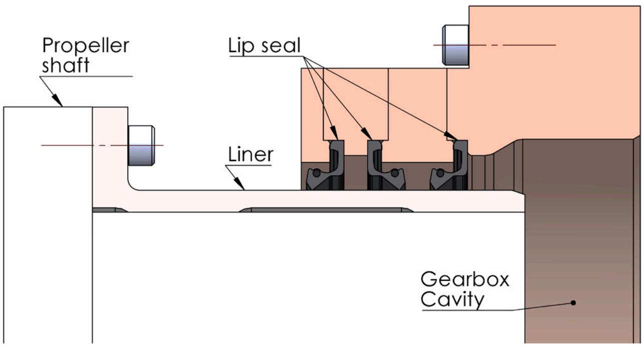

Fig. 1. Example of thruster lip seal system.

former was used to calculate the contact pressure at the lip, while the latter was used to calculate oil flow velocities, oil pressure distribution, and flow cavitation. The frictional torque and pumping rate of the studied lip seals were calculated using the models and verified experimentally [7–15]. Subsequent models were more advanced; some calculated the radial and tangential deformation of the lip at every step [16–20], and some calculated the frictional heat and contact temperature [14,19–21]. Some models considered viscosity dependence on pressure and temperature [20,22], non-Newtonian behavior [23], or the transient behavior of lip seals [18,24–26]. In recent models, the flow factors method was adapted to solve the fluid dynamics part [17], lip seals were modeled as a lumped parameter system [27], and the effects of material aging [28,29] and wear [22,30–33] on lip seal behavior were studied. The numerical models provide insights into the physical phenomena at the contact. However, they have some limitations, such as the need for experimental verification, the limited applicability to the tested seal, and that some models are verified against reversely installed seals. A seal is reversely installed to measure leakage and verify the model. However, this reduces the measured frictional torque [34,35]. Although marine lip seals share some similarities with those studied in the models, their behavior cannot be reliably predicted by such models without experimental verification due to differences, such as the larger diameter, harder rubber compound, different lip geometry, and different structural support methods, i.e., compression fit instead of a metallic L-bracket. In addition, recent lip seal studies focus on numerical models, rather than focusing on lip seal behavior under different operating conditions, e.g., published literature on the behavior of the frictional torque with increasing pressure is limited.

The critical nature of marine lip seal failure, their constant leakage during operation, the scarcity of published research on the behavior of marine lip seals, and the increasing demand for a condition monitoring system of lip seals form the motivation of this study. Condition monitoring can be challenging in marine thrusters due to limited space, harsh operating environment, limited and difficult measurement methods of the condition of the seals, and most importantly, a lack of an understanding of their behavior.

This work aims to expand the limited research on marine thruster lip seals. To the best knowledge of the authors, it comprises of the work of Borras et. al. [36–39] who investigated one sample of a 200 mm fluoroelastomer (FKM) marine lip seal under 12 operating conditions, and a previous work by the authors [40] that studied the behavior of one sample of a 300 mm NBR lip seal under 7 operating conditions. Otherwise, the existing body of research focuses on smaller diameter lip seals (60–100 mm). The present study aims to bridge this gap and expands the authors' previous work [40] by experimentally investigating the behavior of 3 samples of a 300 mm NBR marine lip seal under a comprehensive, 27 sets of typical operating conditions, to establish the behavior of the tested seal. The 300 mm diameter is commonly used in thrusters of interest to the present study. To the best knowledge of the authors, this is the largest lip seal diameter studied in literature, with a higher hardness than most seals in literature, and with a fully flooded oil cavity, which is not common in literature. The viscous torque from the fully flooded oil cavity was accounted for in the analysis. The contact pressure of the lip seal was measured under different sealed pressures. The behavior of the seal was characterized by measuring the frictional torque and the subsurface temperature, using a robust method for the latter. The measurements demonstrated sensitivity to changes in the operating conditions and can be used as the basis of a condition monitoring system for marine thruster seals. Finally, the wear of the lip seal was measured, and its total life was estimated.

2. Materials and methods

In the test sequence, the frictional torque and subsurface temperature of a marine thruster lip seal (n = 3) were measured under 27 different parameter combinations of oil temperature, oil pressure, and rotational speed. The methods are explained in the following subsections. A purpose-built test device was constructed and used for the experimental measurements. The test was followed by experimental and numerical analyses to study the tribological behavior of the tested lip seal.

2.1. Lip seal and liner

In this paper, a marine lip seal and shaft liner from a marine lip seal package were studied. The lip seal was made from Nitrile Butadiene Rubber (NBR), had an 80 Shore A hardness, a garter spring, a nominal diameter of 300 mm, and an interference fit of 4.5 mm for a new seal without the spring. The lip seal had an outer diameter of 345 mm, an inner diameter of 291 mm, and a width of 18 mm. Fig. 2 shows an

Fig. 2. A picture of a cut, unloaded lip seal.

unloaded lip seal. The lip seal was compressed by two housing rings that provided structural support. The liner was made from stainless steel, was hard coated with tungsten carbide, and had an outer diameter of 300 mm. The liner was made to fit a 280 mm propeller shaft, with a close fit and an O-ring groove. Multiple holes were drilled into the inner surface of the liner to place a thermocouple near the contact surface, but only one was used. The holes were 0.5 mm beneath the contact surface, were flat ended, and had a diameter of 1.5 mm. The temperature at this location is expected to be very close to the contact temperature. The hole was filled with copper paste and the thermocouple was tightly placed inside the hole and connected to a wireless transmitter, both of which rotated with the liner. All seals were tested at the same axial position on the liner, which corresponded to a 1.5 mm wide track that coincided with the subsurface thermocouple shown in Fig. 3. The surface roughness of the liner was measured before and after each test to ensure similar test conditions, and no change was observed. The liner was placed on a solid shaft made from Fe 60, with a diameter of 280 mm. The solid shaft closely simulated the thermal aspects of a thruster.

2.2. Test bench

A test bench was constructed to study large diameter marine lip seals. An earlier iteration of the test bench is described in [40]. A schematic of the test bench is shown in Fig. 3. The test bench was constructed on a lathe, which was leveled to be horizontal within ± 0.03°. The shaft and shaft liner were fixed to the lathe chuck and aligned to within 0.06 mm of total dynamic runout. The lip seal and the seal housing were attached to a stationary shaft, which was supported by two radial air bearings that were fixed to the lathe carriage. A thrust air bearing was attached to the tailstock, and mated with a plate connected to the stationary shaft to provide axial support against oil pressure. The air bearings had negligible friction. The seal housing consisted of three parts: two housing rings that fixed the lip seal in place, which were attached to the flanged oil cavity. The lip seal was aligned to the rotation axis of the liner using a dial gauge. In all tests, the axial and radial misalignments were less than 0.2 mm. A load cell was used to prevent the rotation of the lip seal and to measure the frictional load via a rod connected between one of the seal housing bolts and the lathe rails, as shown in Fig. 4, and aligned to be vertical within ± 0.15°. The frictional torque was calculated by multiplying the frictional load by the lever arm.

The test bench was equipped with multiple control methods. A Variable Frequency Drive (VFD) was connected to the lathe motor and controlled the rotational speed to within ± 1 RPM. The rotational speed of the liner was measured using a non-contact tachometer. The oil temperature in the seal housing was measured from three different locations using K-type thermocouples. Two thermocouples were placed

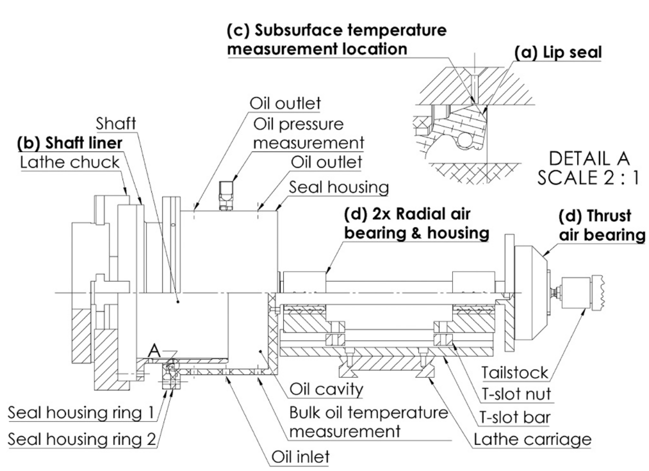

Fig. 3. Schematic drawing of the test bench. (a) Lip seal. (b) Shaft liner. (c) Subsurface temperature measurement location. (d) Air bearings.

near the garter spring of the lip seal, while the third was placed in the oil bulk inside the housing. One of the near-lip thermocouples was connected to a PID controller which controlled the oil heater and maintained the near-lip oil temperature within ± 0.3 °C or less. The oil was heated by three adhesive silicone heating pads with a power of 700 W each. The heating pads were placed on the outer surface of the oil tank to prevent direct contact between the heating pads and the oil, which reduced the possibility of burning the oil. The tank was filled with approximately 80 liters of oil before the tests started. The oil level was above the highest oil hose connection to the tank, to avoid oil aeration. This amount varied during the tests as the oil filled the seal housing and the hoses, and due to the thermal expansion of the oil.

The tank contained about 20 liters of air at room temperature before the start of the test, to account for the volumetric thermal expansion of the oil. A pneumatic line was connected to the top of the tank, which was pressurized with a PID-controlled electro-pneumatic regulator, the input signal of which came from the measured pressure in the seal housing. The oil was circulated via two helical gear pumps, each controlled by a VFD. One pump circulated the oil within the tank at 15–20 liters per minute to maintain a uniform oil temperature, while the other pump circulated the oil through the seal housing at 10–12 liters per minute. The oil was filtered through a 10 μm filter on the discharge line of each pump. The flow rate did not affect the measured frictional torque.

2.3. Test sequence

Each seal was assembled and aligned to less than 0.2 mm of radial and axial misalignments. After alignment, the seal and the liner were coated with oil, and the seal was axially moved onto the liner to the location of the subsurface thermocouple. Afterwards, the oil cavity was filled with oil and the shaft rotation was started. The seal was then moved axially forward and backward to ensure that it was located at the location of the thermocouple. This location corresponded to the highest observed subsurface temperature at steady state conditions. The running-in of the seals was done for 100 h at a rotational speed of 200 RPM, an oil temperature of 40 °C, and an oil pressure of 0.03–0.08 bar. This oil pressure was due to oil circulation.

After the running-in, the test sequence started. It consisted of three parameters: oil temperatures of 40, 50, and 60 °C; oil pressures of 0.1, 0.2, and 0.3 bar; and rotational speeds of 100, 200, and 300 RPM. The rotational speeds corresponded to sliding speeds of 1.57, 3.13, and 4.71 m/s, respectively. There were 27 combinations of test parameters, or test points, and the sample size was 3, for a total of 81 tests. At each test point, the measurements of the test parameters and variables – frictional torque and subsurface temperature – were recorded for at least one hour at steady state conditions. There was a sufficiently long interval after a test point change to allow the measurements to stabilize. The sequence of parameter variation was consistent for all tested seals. The measurements at each test point were averaged for a steady state period of one hour for each sample, and then averaged for the three samples.

2.4. Contact pressure measurement

The contact pressure of the seal was measured using Fujifilm Prescale pressure film, which works by imprinting red pigments of varying densities on a film, which correspond to known pressures. The 'LLW' film was used, which had a pressure range of 0.6–2.5 MPa. The contact pressure measurement was taken after the test bench sequence. The seal was moved away from the liner, then a piece of the film was carefully wrapped around the liner and fixed with adhesive tape, ensuring that it conformed to the curvature of the liner. The lip of the seal was coated with a thin oil film and moved axially onto the liner. The loading procedure of the film manufacturer was followed. The seals were pressurized with air at 0.3, 0.2, and 0.1 bar. A measurement was considered successful when the film showed a smooth circumferential line on the

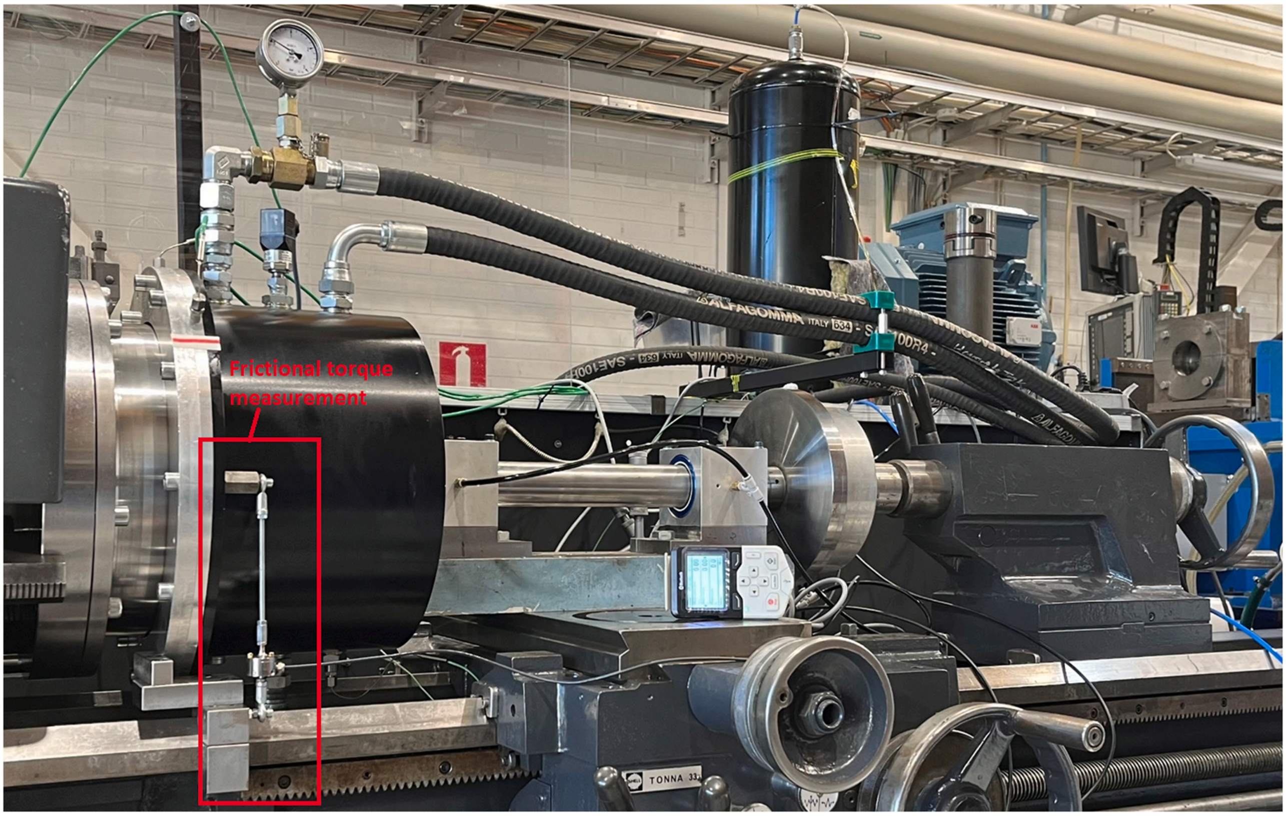

Fig. 4. Picture of the test bench. Frictional load measurement method is enclosed by a red rectangle.

film, with no waviness and with little variation in thickness, as shown in Fig. 5. The contact pressure values were obtained by scanning the films and using the manufacturer's software to digitize the data. The maximum contact pressure value was obtained from the software. The distribution, however, was not obtained from this measurement, since the scanning resolution was 0.15 mm, which was coarse compared to the measured wear track widths.

The pressure distribution was estimated by utilizing the pressure distribution profile of Guo et. al. [41]. The distribution was scaled with the maximum contact pressure from the Fujifilm measurement, and with the measured contact width. In this paper, the wear track width was used as the contact width for the contact pressure distribution at different oil pressures, and in the coefficient of friction calculation. The coefficient of friction was calculated by dividing the frictional torque by the liner radius and total radial force. The total radial force was calculated by integrating the contact pressure distribution along the axial contact width and liner circumference.

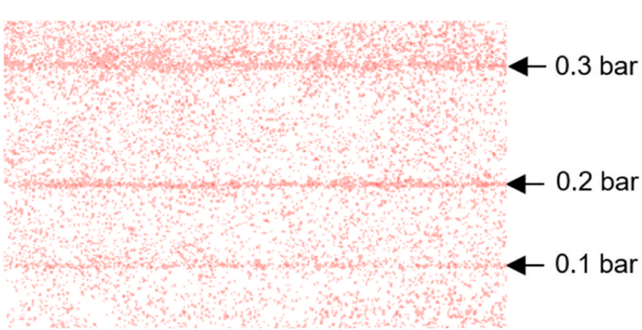

Fig. 5. Scan of pressure film measurement. Pressure values refer to sealed pressure of each trace.

2.5. Wear measurement

The wear track width was measured using an optical microscope with a 10X objective and a focal depth of 18.4 μm. A jig was constructed to hold the entire seal under the microscope, which eliminated the need to cut it, and allowed tilting the seal to ensure that the wear track width was parallel to the focal plane. The contact width was measured 12 times per location, at 12 equally spaced locations on each lip seal. The wear track width was calculated by taking the average of the 144 measurements, and the same value was taken as the contact width.

The worn volume was estimated by tracing the profile of thin strips of the seals on paper using a profile projector with a 10X objective. Three strips were taken from each lip seal, and the profiles of both sides of each strip were traced, scanned, and digitized on SolidWorks, where the worn area and volume were calculated. The profile of an unworn lip seal was examined using the same method, and using a microscope with higher magnification. The unworn profile revealed a sharp corner at the contact. The worn area was estimated by extending lines from the edges adjacent to the wear track, which formed a triangle, as shown in Fig. 6. The wear track widths that were obtained from the profile projector and microscopy were in good agreement.

2.6. Viscous torque estimation

A Computational Fluid Dynamics (CFD) model was needed to estimate the torque produced by the viscous shear of the oil due to rotation, since the seal housing was fully flooded with oil, and the radial gap between the liner and the seal housing was neither narrow enough to assume a linear velocity profile, nor wide enough to assume negligible torque. An axisymmetric, incompressible, unsteady laminar simulation was done using OpenFOAM. The circulation flow of the oil was disregarded, since its effects were considered small compared to the rotation. A summary of the simulation parameters is shown in Table 1. The model was initially verified against two geometries which had an

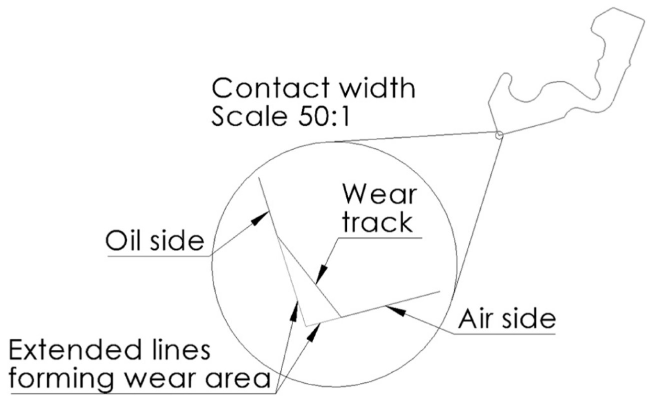

Fig. 6. Traced profile of a lip seal with extended lines forming worn area.

Table 1
Summary of CFD simulation parameters.

Points	289,561
Cells	143,712
Time stepping	Courant number dependent
Courant number	<0.5
Time solver	Euler
Solver scheme (divSchemes)	Gauss linear
Kinematic viscosities	40 °C: 100 mm^2/s
	50 °C: 61.2 mm^2/s
	60 °C: 39.9 mm^2/s
Rotational speeds	100, 200, & 300 RPM
Simulation time	70 s

analytical solution [42,43]: a narrow gap between two rotating disks, and a narrow gap between two rotating cylinders. The torque from each simulation was compared to its corresponding analytical solution and found to be in good agreement. This verification ensured that the numerical solution method was sound.

A mesh sensitivity analysis was conducted to minimize the number of mesh elements required to resolve the boundary layers and was aborted when the calculated viscous torque changed by less than 5 %. The axisymmetric geometry and a snippet of the final mesh is shown in Fig. 7. Nine simulations were done for three speeds and three viscosities that correspond to the oil temperatures. The shear stress values from each simulation were stored for a total of 70 s and postprocessed in MATLAB. The shear stress was numerically integrated over each wall and multiplied by the surface area of each element and its corresponding moment arm to obtain the total viscous torque.

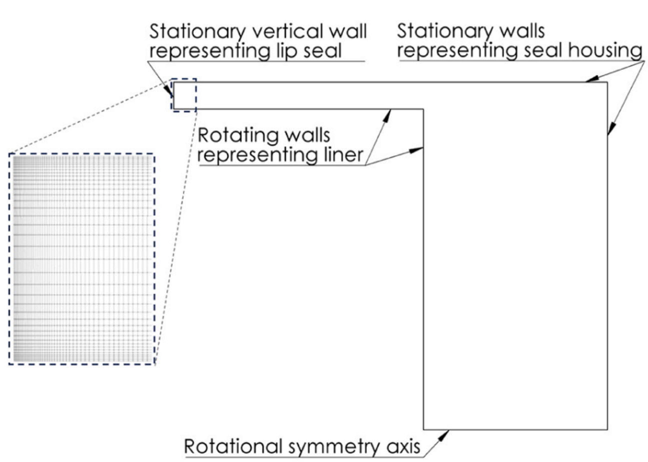

Fig. 7. Schematic of axisymmetric geometry and a snippet of the mesh.

3. Results

3.1. Frictional torque and subsurface temperature

The steady state measurements of the frictional torque and subsurface temperature are shown in Fig. 8, where each point represents the mean value of the three seal samples at a given test point. Generally, an increasing oil temperature decreases the frictional torque and increases the subsurface temperature. An increasing oil pressure increases the frictional torque and slightly increases the subsurface temperature. An increasing rotational speed increases the subsurface temperature, but does not have a clear effect on the frictional torque. The effect of increasing rotational speed on frictional torque and subsurface temperature is described by the linear regression equations shown in Fig. 8.

3.2. Contact width, wear volume, and wear rate

The micrographs of the tested seals show the wear tracks. Seal 1 experienced a degree of thermal glazing at various locations around the circumference of the lip, as shown in Fig. 9a. The glazing is evident when compared to the sealing edge of lip seals 2 and 3, shown in Fig. 9b and Fig. 9c, respectively. The sealing edges of seals 2 and 3 show a non-glazed rough surface and reveal the filler, which is likely metallic and can be seen as the brightly colored specs in the figures. A summary of the wear measurements is shown in Table 2. Seal 1 had the longest running time, the widest wear track, and the highest wear volume. Seals 2 and 3 had similar running times, wear track widths, and wear volumes. The wear rate, mean $\pm$ SD, of the three seals was 0.031 $\pm$ 0.001 mm^3/hour. A linear regression of the wear volume and running time gives the following equation for estimating the wear volume: $V = 0.034t - 0.536$, where V is the wear volume in mm^3, and t is the running time in hours. The linear regression had an $R^2 = 0.9993$. The life of the seal was estimated to be 50,000 h, assuming seal failure occurs when the contact width reaches 3 mm, which corresponds to a wear volume of 1700 mm^3.

3.3. Contact pressure and coefficient of friction

The measured maximum contact pressures of the seals, shown in Table 3, were consistent across all seals at different sealed pressures. The contact pressures and measured wear track widths were used to scale the pressure distribution of Guo et. al. [41]. The pressure distributions were integrated over the total contact area to obtain the resultant contact force and calculate the coefficients of friction, which are shown in Fig. 10.

3.4. Viscous torque

The calculated viscous torques are shown in Fig. 11. The viscous torque increased with increasing rotational speeds and decreasing oil temperatures. At higher temperatures, the Taylor vortices had a periodic behavior, where one period was 0.6–0.8 s. In those cases, the torque was calculated by taking the average of multiple oscillations. The amplitude of the oscillation was $\pm$ 2 % of the average value of the torque. An example of the oscillations is shown in Fig. 12 at a speed of 300 RPM and an oil temperature of 60 °C. The viscous torques were subtracted from the measured frictional torque at each test point.

4. Discussion

In the test bench, the seals had consistent behavior. For instance, the frictional torque always increased with increasing oil pressure, which can be explained by the increased radial load. An increase in oil pressure also deforms the lip and may increase the contact width [44], depending on the seal geometry. The radial load increases as well, as shown in Table 3. The separation between the lip and the liner, i.e., the oil film, is

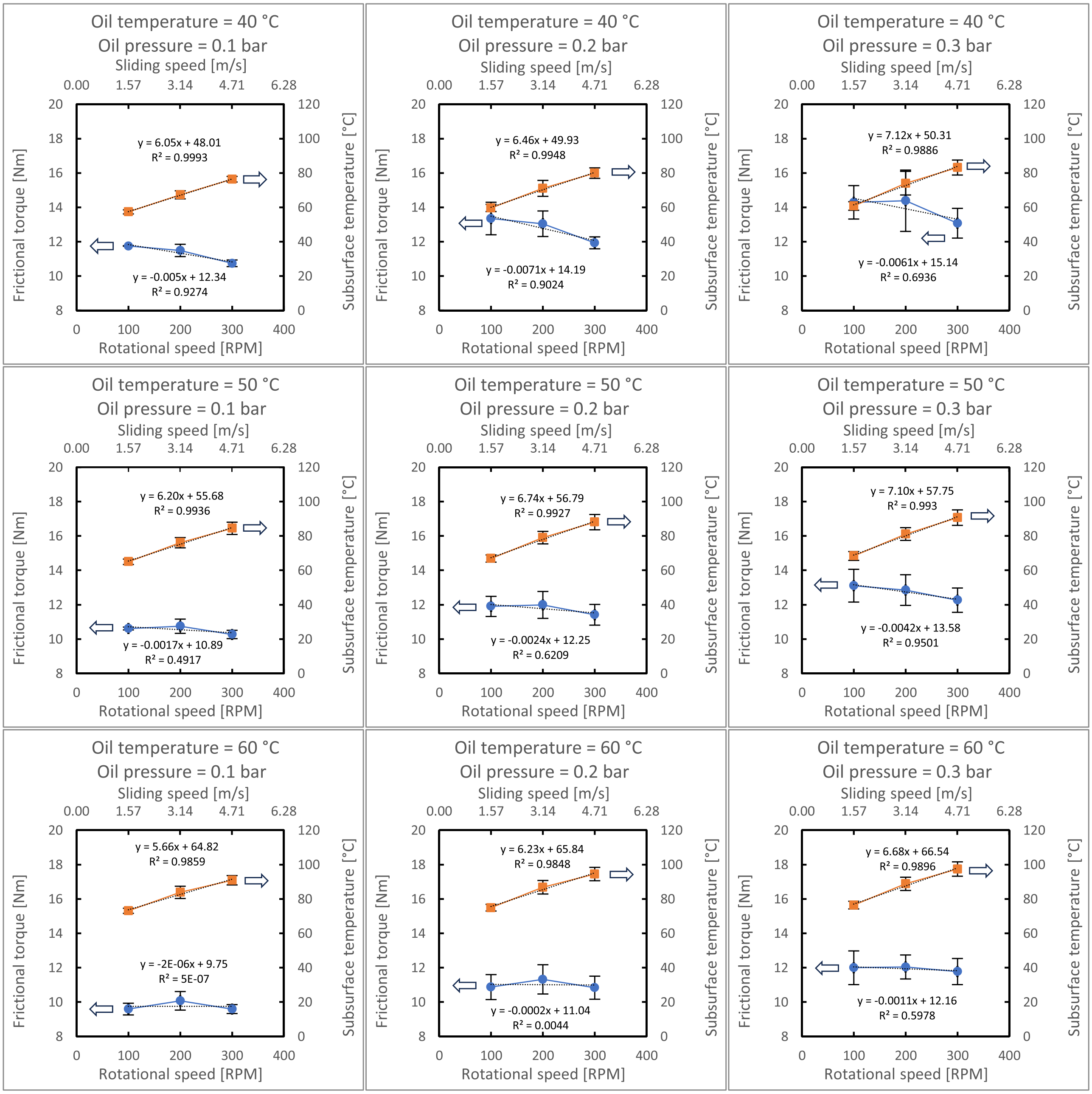

Fig. 8. Frictional torque and subsurface temperature at different operating conditions. Each point is the mean of the three samples and the error bars represent the standard deviation at a given oil temperature, oil pressure, and rotational speed. Each plot shows measurements at one oil temperature, one oil pressure, and three rotational speeds. The arrows point to the vertical axis of each curve.

also affected, since the oil film thickness depends on the balance between the radial load and the oil pressure in the film. Hence, an increase in radial load may reduce the oil film thickness, resulting in an increase in asperity contact, increasing the frictional torque. The results are in accordance with [39,45].

The frictional torque decreased with increasing oil temperature. An increase in oil temperature decreases the elastic modulus of the elastomer and the oil viscosity. The lower elastic modulus results in a lower radial load, which reduces the frictional force due to asperity contact and the coefficient of friction, as shown in Fig. 10. The lower viscosity reduces the viscous component of the frictional torque, but it also reduces the oil film thickness [46], which may increase the asperity contact. However, the results indicate that either the asperity contact did not increase, or that the increase in asperity contact was countered by the lower viscous and radial forces. Since the coefficient of friction always decreased with increasing oil temperature, it is more likely that the decrease in local oil viscosity and oil film thickness was more significant than the increase in asperity contact. The results agree with those of [46]. Theoretically, if the oil temperature increases significantly, the oil film thickness may reduce so much so that asperity contact occurs, leading to an increase in frictional torque. However, this has not been observed in the present study, nor literature, to the best knowledge of the authors.

There was a weak correlation between the frictional torque and the rotational speed. In some cases, it decreased, whereas in others it increased or remained constant. For instance, at an oil temperature of 50 °C and an oil pressure of 0.1 bar, the frictional torque was 10.6 and 10.8 Nm at speeds of 100 and 200 RPM, respectively. The change in torque is small compared to other oil temperatures and pressures in Fig. 8. The subsurface temperature increased from 65.0 °C at 100 RPM

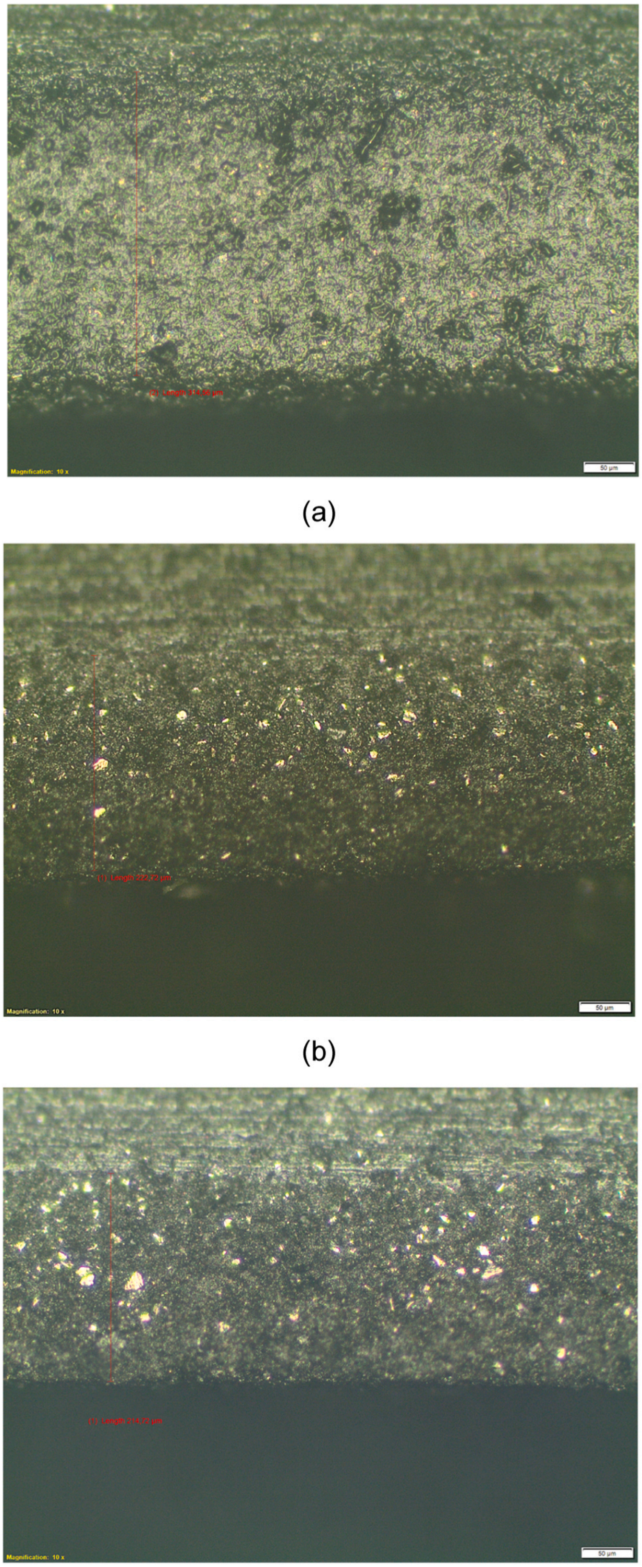

(c)

Fig. 9. Wear tracks of tested seals. The scale at the bottom right corner of each micrograph is 50 μm. Wear track widths are: (a) Seal 1 = 0.32 mm, (b) Seal 2 = 0.22 mm, and (c) Seal 3 = 0.21 mm.

Table 2
Summary of wear measurements.

Parameters	Units	Seal 1	Seal 2	Seal 3
Total running time	Hours	499	191	196
Maximum subsurface temperature	°C	102.2	95.5	94.6
Average wear track width	μm	328	217	214
Wear volume	mm^3	16.2	6.0	5.9
Wear rate	mm^3/hour	0.0325	0.0315	0.0301

Table 3
Maximum contact pressures.

	Maximum contact pressure [MPa]		
Sealed pressure [bar]	Seal 1	Seal 2	Seal 3
0.1	1.02	0.95	1.02
0.2	1.12	1.18	1.13
0.3	1.18	1.22	1.14

to 76.1 °C at 200 RPM, which corresponds to a 34 % decrease in local viscosity. The small increase in frictional torque with higher speed indicates that the increase in hydrodynamic film generation due to the higher speed balances the decrease in film thickness due to the lower viscosity. At 300 RPM; the frictional torque decreases to 10.3 Nm, while the subsurface temperature increases to 84.5 °C. The increase in film thickness due to the higher speed is likely more significant than the reduction in oil film thickness due to lower viscosity, and the lower torque may be attributed to a reduction in asperity contact. While a lower elastic modulus has the same effect, it is less likely to be a significant factor, since the bulk oil temperature was constant across these tests, and the contact temperature only has a local effect on the lip material; most of the radial load of the lip seal comes from its cantilever-shaped geometry, so the effect of the lower elastic modulus would be significant if the oil temperature at the cantilever section changes, which is seen at higher oil temperatures in Fig. 8. The linear regression equations in Fig. 8 demonstrate the variation of the balance between different factors (viscosity, hydrodynamic film generation, asperity contact, and elastic modulus) for a given oil temperature and pressure; in only 3 of the 9 plots, the linear regression of the frictional torque and rotational speed showed high dependence, where R^2 was higher than 0.9. In the other cases, R^2 was less than 0.7, in two of which it was less than 0.1. In the literature, the frictional torque of some seals increased with increasing rotational speed [41], whereas for others, it decreased [39] or remained constant [4,47]. In those studies, the sliding speeds were different, or the seals were reversely installed, both of which have a significant impact on the behavior of the lip seal, and may explain the difference in behavior.

The subsurface temperature increased slightly with increasing oil pressure, which is attributed to an increase in heat generation due to the increase in contact pressure and a possible increase in asperity contact, which are accompanied by an increase in frictional torque. This is in accordance with the findings of [20,21,39,47].

An increasing oil temperature increased the subsurface temperature, which is primarily due to higher frictional heat retention at the contact area, since hotter oil can absorb less frictional heat. Another explanation is that a higher oil temperature reduces viscosity and results in a thinner oil film, which increases the possibility of asperity contact and may increase frictional heating. However, the consistent decrease in frictional torque indicates that this was minimal. The lower film thickness does not necessarily increase frictional torque since it decreases the viscous shear within the film. In addition, the reduced radial load at higher oil temperatures may reduce asperity contact [46]. Therefore, the increase in subsurface temperature with increasing oil temperatures is unlikely to be due to an increase in frictional heating. The results are in agreement with the findings of [22,39,46,47].

The subsurface temperature increased significantly with increasing

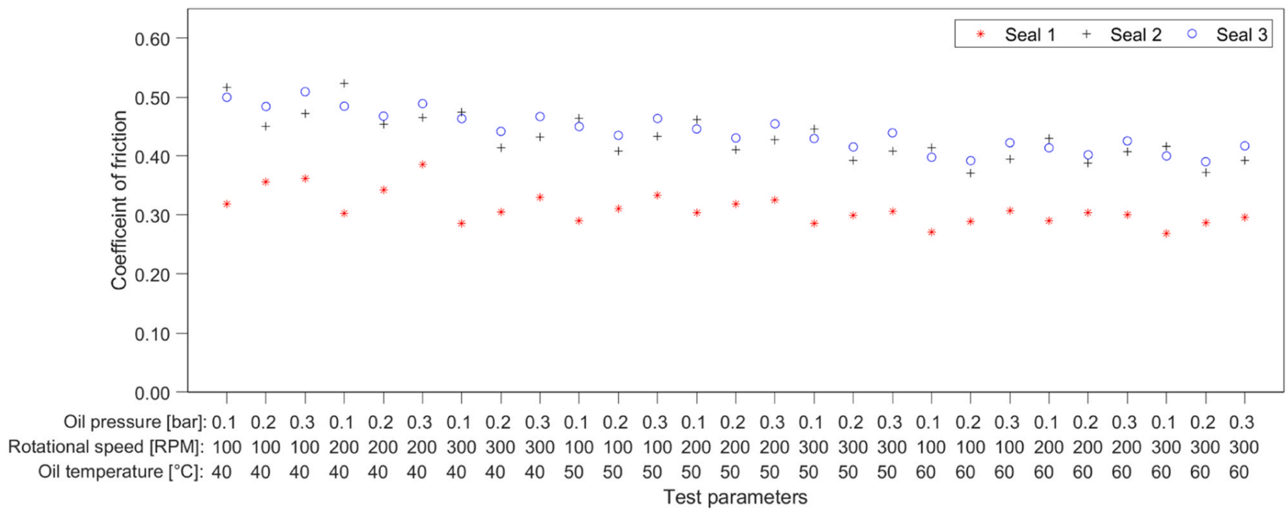

Fig. 10. Coefficients of friction.

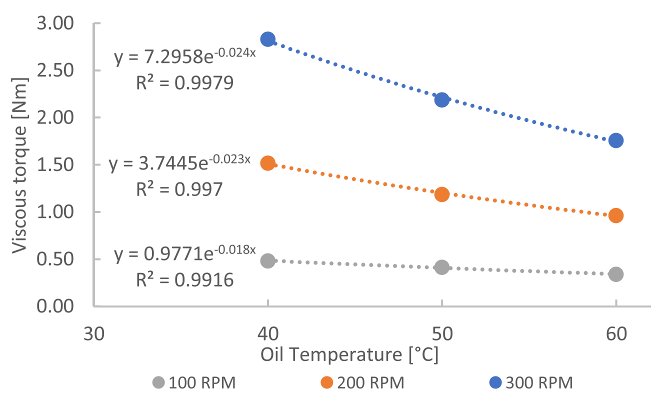

Fig. 11. Viscous torque at different speeds and temperatures.

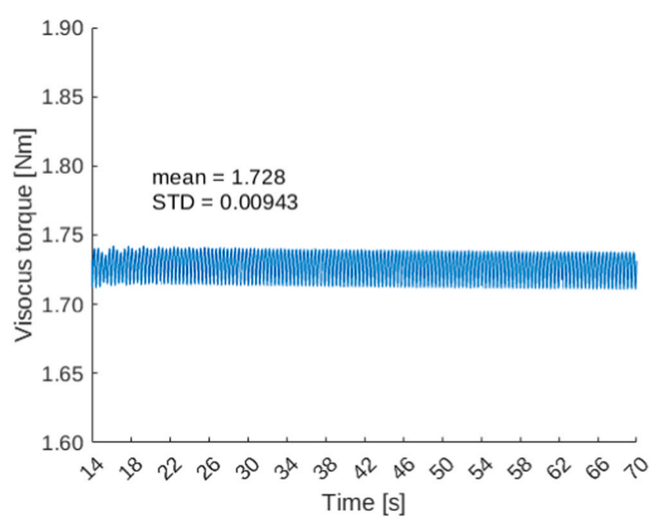

Fig. 12. Oscillations in viscous torque due to Taylor instabilities at 300 RPM and 60 °C.

rotational speed, which is due to the increase in frictional heating at the contact. The results indicate that the increase in subsurface temperature is the net effect of increased viscous shear within the oil film due to higher speed, increased frictional heating due to higher speed, lower oil film thickness due to higher local temperatures, and a possible increase in asperity contact. The results agree with those of [21,33,39,46,48].

The wear of the tested seals was measured by a microscope to obtain the contact width, and by a profile projector to measure the wear area. There was good agreement between the results of both methods. The worn area was triangular, which is due to the manufacturing method wherein the edge of a new lip seal is cut with a sharp tool after the seal is molded. The triangular wear area was also observed by [22,49]. A similar contact width and a lower wear rate were reported in [22], while a larger wear rate was reported in [32]. Differences in the wear rate are expected, since it is affected by the shaft roughness, seal material, seal diameter, and operating conditions. The low standard deviation of the average wear rate demonstrates the similarity between the seal samples and between the tests. The wear of the seal and its life may be estimated with the wear equation, assuming a constant wear rate. The life of the seal was estimated to be 50,000 h, based on results from a yet unpublished study on a failed seal, which had a contact width of 3 mm, corresponding to a wear volume of 1700 mm^3. However, this estimate requires verification with longer wear tests, since the wear rate may vary with running time, especially due to glazing at the contact, which was observed in the relatively short duration of this test. When the seal contact is glazed, the wear rate increases, and a smooth surface develops, which lowers the reverse pumping ability of the seal [19] and may increase leakage.

To calculate the coefficient of friction, the contact pressure distribution must be calculated. This is usually done with an FEM analysis, with many examples in the literature [12,21,33,36,39,41,50–52]. The pressure distributions are typically asymmetric and resemble a parabolic or sinusoidal distribution, or in some cases, a triangle. The point of maximum contact pressure is usually located 20–30 % of the contact width away from the distribution center towards the spring side. Since the pressure distributions in the literature are similar, one could use the profiles of the distributions and scale them accordingly with the maximum contact pressure and contact width to obtain a reasonable estimation of the coefficient of friction, which was done in this study using the measured wear track width and maximum contact pressure. The latter was measured using the Fujifilm method, which has been performed and verified by other researchers [44,53–55]. The coefficients of friction varied between 0.27–0.52, and were of the same order of magnitude as those obtained by other researchers [4,34,39,56]. These values, in addition to the absence of a transfer layer on the liner, indicate that the lubrication regime was likely mixed, and that asperity contact likely occurred. Some numerical models use coefficient of friction values of 0.05–0.1, assuming full hydrodynamic films. Such values may be obtained experimentally with a low viscosity oil and low radial loading [34], although with difficulty since this requires the optimization of many parameters.

The frictional torque measurement was stable during the tests. The measurement had two components: the frictional torque from the lip seal and the viscous torque originating from the lubricant shear in the fully flooded oil cavity. The viscous torque of the lubricant was calculated using a CFD simulation in OpenFOAM. There were some simplifications in the model, such as modeling the lip geometry as a line, and disregarding the circulation flow, since it was an order of magnitude lower than the fluid velocities inside the seal housing due to liner rotation. About 80 % of the viscous torque originated from the shear in the radial gap between the rotating liner and the housing. The simulation results were verified against the radial and axial velocity profiles of similar cases with a similar Reynolds number in [57,58], and were in good agreement.

A sample of a similar seal was tested in a previous article by the authors [40] under seven different operating conditions, albeit with a different oil and using an earlier iteration of the test bench which had a different thrust bearing. The frictional torque in [40] was higher than that in the present study. This was due to two reasons. Firstly, the reported torque values in [40] included the viscous torque from the lubricant shear in the oil cavity. Secondly, the lubricating oil was filtered through a fine mesh filter of 5 μm, which likely filtered out the antifoam silicone additive in the oil. The presence of foam in the oil was visually confirmed. An oil analysis showed that the test oil in [40] had a high tendency to foam: it had an ASTM D892 foaming tendency Sequence 1 of 40/310 mL/mL, in contrast to the unfiltered oil, which had a foam tendency of 0/0 mL/mL. If the contribution of the viscous oil torque was removed from the measured frictional torque in [40], it would still be higher than the present results. This is attributed to the lack of antifoam in the oil, which increases the chance of foaming, and results in a larger variation in frictional torque at steady state conditions. In another unreported test with foamy oil, there was a transfer layer on the liner after a few days of testing, which indicates a different wear mechanism when foam is present in the oil. The presence of foam likely increased cavitation in the contact area, which increased the wear of the seal and may have resulted in starved lubrication. The subsurface temperature with foamy oil was higher as well, which supports the possibility of starved lubrication.

The present study extensively focuses on the change of lip seal behavior at different operating conditions by testing three samples under a comprehensive combination of different operating conditions. Each sample was tested under 27 operating conditions, and the sequence of change was repeated for all seals. The standard deviation in operating conditions and measured variables was less than 2 % of the mean in all tests. Therefore, the observed change in behavior is highly likely to be due to actual changes in the lubrication affected by changes in the operating conditions. Furthermore, the measurement method of subsurface temperature in the present study provides a better approximation of the contact temperature, due to the proximity of the measurement location to the contact without disturbing the contact.

This study provides insight into the behavior of large diameter lip seals. From a scientific perspective, it studies a lip seal with a diameter larger than those studied in the literature, which is made from a harder material, and continues the previous work of the authors [40]. Most of the studied NBR lip seals in literature have a nominal diameter of 60–100 mm, and frictional torques ranging from 0.5–3.0 Nm, while the frictional torque of the 300 mm lip seal in the present study was 9.6–14.4 Nm. From a practical perspective, the results demonstrate the viability of the measurement methods of frictional torque and subsurface temperature, the sensitivity of the two measurements to different operating conditions, and their usability in condition monitoring. The subsurface temperature method may be viable for use in a marine thruster, since it does not interfere with the fixture method of seal packages nor with the contact.

Possible experimental sources of error include the following: in the test bench, it is likely that the axial location of the lip seal varied slightly between or during the tests due to different loading conditions. The material of the lip seals may have aged for different periods in air and oil. The exact test durations varied slightly between the tests. The contact pressure measurement may have had errors due to possible slip-stick friction with the seal, in addition to the ± 10 % accuracy of each measurement, and the differences in temperature, humidity, and light exposure. The misalignments differed slightly between tests, which may have affected the local contact conditions. The numerical errors include those of the viscous torque simulation, which stemmed from resolving the boundary layer with an optimized mesh size, the numerical solution method, and some of the simplifications. In the contact pressure calculation, the shape of the pressure distribution was taken from the literature, and the applicability to the presently studied seal may be limited. In the calculation of wear, the profiles of the lip seals were traced, which involved approximations of the exact slopes of the traced lines and curves, which can affect the computed wear volume.

5. Conclusion

In this paper, an NBR marine lip seal ($n = 3$) was tested under 27 combinations of realistic operating conditions. Based on the measurements of the frictional torque and the calculation of the coefficient of friction, the seals likely operated in the mixed lubrication regime. The subsurface temperature measurement method in this paper was proven robust, as it gave a close approximation of the contact temperature due to its proximity to the contact without disturbing the contact. In some tests, the subsurface temperature was close to 100 °C, and evidence of thermal glazing was found, which indicates a tendency of higher wear and a larger risk of leakage in marine thrusters. This work provides measurement values that may be used to develop or verify numerical models.

The behavior of a marine lip seal was assessed under a comprehensive test program of 27 operating conditions with 3 samples. The tests demonstrated that the subsurface temperature increases with an increasing oil temperature, oil pressure, and rotational speed to varying degrees, as described with mapping relationships. The results agree with the current body of research. As for the frictional torque, its behavior was in agreement with the published research in its increase with increasing oil pressure and decrease with increasing oil temperature. Its behavior with increasing speed depended significantly on the oil pressure and temperature and is described with mapping relationships.

The wear of the tested seal was measured and quantified, and a wear rate was obtained. Based on the calculated wear rate, the life of the tested seal was estimated to be 50,000 h. However, longer wear tests are needed to verify this estimate.

Statement of originality

I, Omar Morad, the Corresponding Author, declare that this manuscript is original, has not been published before and is not currently being considered for publication elsewhere. I can confirm that the manuscript has been read and approved by all named authors and that there are no other persons who satisfied the criteria for authorship but are not listed. I further confirm that the order of authors listed in the manuscript has been approved by all of us. I understand that the Corresponding Author is the sole contact for the Editorial process and is responsible for communicating with the other authors about progress, submissions of revisions and final approval of proofs.

CRediT authorship contribution statement

Omar Morad: Writing – review & editing, Writing – original draft, Visualization, Validation, Software, Resources, Project administration, Methodology, Investigation, Funding acquisition, Formal analysis, Data curation, Conceptualization. **Raine Viitala:** Writing – review & editing, Supervision, Resources, Project administration, Funding acquisition, Conceptualization. **Vesa Saikko:** Writing – review & editing, Validation, Supervision, Resources, Project administration, Methodology.

Declaration of Competing Interest

The authors declare that they have no known competing financial interests or personal relationships that could have appeared to influence the work reported in this paper.

Data availability

Data will be made available on request.

Acknowledgements

The research was funded by Academy of Finland (AI-ROT, grant number 335717), Business Finland (Power Beyond, grant number 2534/31/2022), and Kongsberg Maritime Finland Oy.

References

[1] Lundberg, J., Undocumented oil leakages: a study about stern tube seals and leakages; 2021.
[2] Jagger, E.T. Study of the lubrication of synthetic rubber rotary shaft seals. In: Proc. conf. on lubrication and wear, institute of mechanical engineers; 1957.
[3] Jagger ET. Rotary shaft seals: the sealing mechanism of synthetic rubber seals running at atmospheric pressure. Proc Inst Mech Eng 1957;171(1):597–616.
[4] Müller, H.K. , Ott, G.W. Dynamic sealing of rubber rotary shaft seals. In: Proceedings of the tenth international conference on fluid sealing; 1984.
[5] Qian D. The sealing mechanism and design factors of radial lip seals for crankshafts. Neiranji Gongsheng/Chin Intern Combust Engine Eng 1984;5:10–3.
[6] Salant RF. Numerical analysis of the flow field within lip seals containing microundulations. J Tribol 1992;114(3):485–91.
[7] Gabelli A, Poll G. Formation of lubricant film in rotary sealing contacts: part i—lubricant film modeling. J Tribol 1992;114(2):280–7.
[8] Poll G, Gabelli A. Formation of lubricant film in rotary sealing contacts: part ii—a new measuring principle for lubricant film thickness. J Tribol 1992;114(2):290–6.
[9] Salant RF, Flaherty AL. Elastohydrodynamic analysis of reverse pumping in rotary lip seals with microundulations. J Tribol 1994;116(1):56–62.
[10] Salant RF, Flaherty AL. Elastohydrodynamic analysis of reverse pumping in rotary lip seals with microasperities. J Tribol 1995;117(1):53–9.
[11] Salant RF. Elastohydrodynamics of the rotary lip seal. Lubr Sci 1997;9(2):111–25.
[12] Salant RF. Modelling rotary lip seals. Wear 1997;207(1):92–9.
[13] Salant RF. Theory of lubrication of elastomeric rotary shaft seals. Proc Inst Mech Eng, Part J J Eng Tribology 1999;213(3):189–201.
[14] Day K, Salant RF. Thermal elastohydrodynamic model of a radial lip seal—part I: analysis and base results. J Tribol. 1999;121(1):1–10.
[15] Shi F, Salant RF. A mixed soft elastohydrodynamic lubrication model with interasperity cavitation and surface shear deformation. J Tribol 1999;122(1):308–16.
[16] Shen D, Salant RF. Elastohydrodynamic analysis of the effect of shaft surface finish on rotary lip seal behavior. Tribol Trans 2003;46(3):391–6.
[17] Rocke AH, Salant RF. Elastohydrodynamic analysis of a rotary lip seal using flow factors. Tribol Trans 2005;48(3):308–16.
[18] Shen D, Salant RF. A transient mixed lubrication model of a rotary lip seal with a rough shaft. Tribol Trans 2006;49(4):621–34.
[19] Hajjam M, Bonneau D. Influence of the roughness model on the thermoelastohydrodynamic performances of lip seals. Tribol Int 2006;39(3):198–205.
[20] Maoui A, Hajjam M, Bonneau D. Analysis of three-dimensional non-axisymmetric elastic effects of the lip on the thermoelastohydrodynamic radial lip seal behaviour. Proc Inst Mech Eng, Part J J Eng Tribology 2007;221(8):859–68.
[21] Maoui A, Hajjam M, Bonneau D. Numerical analysis of thermoelastohydrodynamic behavior of elastomer radial lip seals. J Tribol 2008;130(2).
[22] Frölich D, Magyar B, Sauer B. A comprehensive model of wear, friction and contact temperature in radial shaft seals. Wear 2014;311(1):71–80.
[23] Hajjam M, Dominique B. Non-Newtonian effects on elastohydrodynamic behaviour of rotary lip seals. Proc Inst Mech Eng, Part J J Eng Tribology 2006;220(2):79–85.
[24] Salant RF. Elastohydrodynamic model of the rotary lip seal. J Tribol Trans ASME 1996;118(2):292–6.
[25] Salant RF. Rotary lip seal operation with an ingested meniscus. J Tribol Trans ASME 1997;119(1):205–10.
[26] Salant RF. Analysis of the transient behavior of rotary lip seals - fluid mechanics and bulk deformation. Tribol Trans 1998;41(4):471–80.
[27] Mazza L, Belforte G. Analytical/experimental study of the contribution of individual seals to friction force in pneumatic actuators. J Tribol Trans ASME 2017;139(2).
[28] Guo F, Jia X, et al. The effect of aging during storage on the performance of a radial lip seal. Polym Degrad Stab 2013;98(11):2193–200.
[29] Guo F, Jia X, et al. The effect of aging in oil on the performance of a radial lip seal. Tribol Int 2014;78:187–94.
[30] Guo F, Jia X, et al. The effect of wear on the performance of a rotary lip seal. J Tribol 2014;136(4).
[31] Liu D, Wang S, et al. Numerical analysis of rotary lip seal performance deterioration. In: Proceedings of the IEEE eleventh conference on industrial electronics and applications (ICIEA) 2016.
[32] Liu D, Wang S, Zhang C. A multiscale wear simulation method for rotary lip seal under mixed lubricating conditions. Tribol Int 2018;121:190–203.
[33] Grün J, Feldmeth S, Bauer F. Wear on radial lip seals: a numerical study of the influence on the sealing mechanism. Wear 2021;476:203674.
[34] Hirano F, Ishiwata H, Kambayashi H. Friction and sealing characteristics of oil seals. in: Proceedings of the first Intl. Conf. on Fluid Sealing 1961.
[35] Kammüller, M., Zur abdichtwirkung von radial wellendichtringen (Dr-Ing thesis). Universität Stuttgart, 1986.
[36] Borras FX, de Rooij MB, Schipper DJ. Misalignment-induced micro-elastohydrodynamic lubrication in rotary lip seals. Lubricants 2020;8(2):19.
[37] Borras FX, de Rooij MB, Schipper DJ. Misalignment-induced macro-elastohydrodynamic lubrication in rotary lip seals. Tribol Int 2020;151:106479.
[38] Borras FX, Bazrafshan M, et al. Stern tube seals under static condition: a multi-scale contact modeling approach. Proc Inst Mech Eng Part J J Eng Tribology 2020;235(1):181–95.
[39] Borras FX, van den Nieuwendijk R, et al. Stern tube seals operation: a practical approach. Adv Mech Eng 2021;13(2):1–14.
[40] Morad O, Saikko V, Viitala R. Performance characterization of marine lip seals: contact temperature and frictional torque. Wear 2023;523.
[41] Guo F, Jia X, et al. A mixed lubrication model of a rotary lip seal using flow factors. Tribology Int 2013;57:195–201.
[42] Bird RByron, Edwin WES, Lightfoot N. Transport phenomena, revised 2nd edition. 2nd edition. John Wiley & Sons, Inc; 2009.
[43] Childs PRN. Rotating flow. In: Childs PRN, editor. Rotating flow. Oxford: Butterworth-Heinemann; 2011. p. 81–247.
[44] Lee C-Y, Lin C-S, et al. Simulation and experimentation on the contact width and pressure distribution of lip seals. Tribol Int 2006;39(9):915–20.
[45] Jia X, Guo F, et al. Effects of the radial force on the static contact properties and sealing performance of a radial lip seal. Sci China Technol Sci 2014;57(6):1175–82.
[46] Yan C, Jia X, et al. Influence of oil temperature on the lip seal's performance. Tribol Trans 2019;62(5):739–46.
[47] Jia X, Jung S, et al. Numerical simulation and experimental study of shaft pumping by laser structured shafts with rotary lip seals. Tribol Int 2011;44(5):651–9.
[48] Wilke M, Wollesen V, Estorff Ov. Erarbeitung einer dynamischen Prüfmethode auf der Basis einfacher Prüfkörper zur Beurteilung von Öl-Elastomer-Paarungen unter den Aspekten Reibung und Verschleiß. DGMK Forsch 2011;664.
[49] Wenk JF, Stephens LS, et al. A multi-scale finite element contact model using measured surface roughness for a radial lip seal. Tribol Int 2016;97:288–301.
[50] Calonius O, Pietola M. Explicit finite element analysis of tracking capability of rotary face seal for industrial fluid power applications. In: Proceedings of the JFPS international symposium on fluid power 2005;2005.
[51] Silvestri, M., Prati, E., Tasora, A., Radial lip seals efficiency under dynamic operating conditions; 2006.
[52] Grün J, Feldmeth S, Bauer F. Wear on radial lip seals: a numerical study of the influence on the sealing mechanism. Wear 2021;476.
[53] Belforte G, Conte M, et al. Experimental and numerical evaluation of contact pressure in pneumatic seals. Tribol Int 2009;42(1):169–75.
[54] Belforte G, Conte M, Mazza L. Low friction multi-lobed seal for pneumatic actuators. Wear 2014;320:7–15.
[55] Conte M. Interaction between seals and counterparts in pneumatic and hydraulic components 2009.
[56] Engelke T. Elastomer-Schmierstoff-Kombination auf das Betriebsverhalten von Radialwellendichtringen 2011.
[57] Merbold S, Hamede MH, et al. Flow regimes in a very wide-gap Taylor-Couette flow with counter-rotating cylinders. Philos Trans A Math Phys Eng Sci 2023;381(2246):20220113.
[58] Schouveiler L, Le Gal P, Chauve MP. Instabilities of the flow between a rotating and a stationary disk. J Fluid Mech 2001;443:329–50.